INVESTIGATION OF VELOCITY DISTRIBUTION IN CHANNELS AND CHAMBERS OF THE ELECTROSTATIC PRECIPITATOR AT TPP NIKOLA TESLA UNIT A1

by

Zoran J. MARKOVIĆ[a*], Milić D. ERIĆa, Predrag Lj. STEFANOVIĆ[a], Ivan M. LAZOVIĆ[a], Aleksandar R. MILIĆEVIĆ[a], Marko V. MANČIĆ[b], Milica JOVČEVSKI[b], and Rastko D. JOVANOVIĆ[a]

[a] VINČA Institute of Nuclear Sciences, National Institute of the Republic of Serbia, University of Belgrade, Belgrade, Serbia
[b] Faculty of Mechanical Engineering, University of Niš, Niš, Serbia

Original scientific paper
https://doi.org/10.2298/TSCI230816244M

To achieve the optimum dust removal performance of an electrostatic precipitator, the flue gas should be distributed uniformly over its vertical cross-section. The flow in the upstream flue gas ducts has a significant influence on the downstream gas distribution in the chamber of the precipitator. This paper presents the results of homogeneity assessment of velocity distribution in the ducts and vertical cross-sections of the electrostatic precipitator of Unit A1 at the Nikola Tesla thermal power plant in Obrenovac. The measurements confirmed that the reconstruction of the vertical chamber at the front of the precipitator, which was carried out during the overhaul in 2020, effectively solved the problem of the original asymmetric arrangement of the vertical flue gas ducts. Nevertheless, the analysis revealed poor homogeneity of the flow field through the chambers. Therefore, additional measures must be taken to increase the dust removal efficiency of the precipitator.

Key words: *electrostatic precipitator, velocity measurements, flow homogeneity assessment*

Introduction

When summarizing the different disease domains (neuronal, respiratory, cardiovascular, and oncological) affected by exposure to PM, NO_2, SO_2, CO_2, and O_3 pollution, the PM was found to be associated with all of the mentioned diseases [1]. Taking into account the fuel production chain, the production of required infrastructure and waste disposal, the total cost of environmental damage caused by PM emissions differs significantly between Serbian coal-fired power plants [2]. When distributing the total damage among the individual impact categories, the Nikola Tesla A thermal power plant (TPP) in Obrenovac reaches the highest absolute value for the damage to human health, with the relative contribution of PM emissions to the life cycle damage costs being 6%. In order to separate PM from the flue gas, one of the two oldest units of this power plant, Unit A1, is equipped with two-chamber dry electrostatic precipitators (ESP). According to the results of periodic measurements carried out in 2016 and 2018, *i.e.* continuous measurements in 2017, PM emission from Unit A1 exceeded the emission limit value of 50 mg/Nm^3, increasing over the years. The general overhaul of the plant is sched-

* Corresponding author, e-mail: zoda_mark@vin.bg.ac.rs

uled for 2022/2023, and it is expected to be shut down for an extended period (12 months). It is planned to undertake adequate interventions at the ESP to reduce PM emissions. Prior analysis based on appropriate measurements was asked to identify the limits to achieving the required high dust removal efficiency and propose measures to eliminate them. The uniformity of the flue gas-flow in the chamber of ESP significantly affects its efficiency [3]. Since the upstream flow through the inlet ducts influence downstream flow through the ESP chamber [4], it was necessary to evaluate the uniformity of the flow in the ducts as well as in the chambers of ESP.

Due to the enlargement of the ESP chamber of Unit A1, (fig. 1, pos. 10), during the reconstruction in 2006, the axis of the existing horizontal flue duct, fig. 1, pos. 1, at the exit of the rotating regenerative (Ljungström) air preheaters (RAPH) was shifted by 550 mm with respect to the axis of the ESP chamber. This resulted in an asymmetric arrangement of two vertical flue ducts, fig. 1, pos. 4, with respect to the vertical plane of symmetry of the ESP chamber. Moreover, the asymmetry of the flow in the ESP chamber is aggravated by the asymmetrical position of the outlet duct, fig. 1, pos. 14, with respect to the axis of the chamber.

Measuring gas-flow through pipes/ducts is a problem of great importance in the process and gas/oil production/transmission industry [5]. A number of researchers have looked at different solutions and meters (differential head, variable-area, velocity flow, mass-flow, positive displacement, electromagnetic, ultrasonic) to determine the suitability of methods and instruments in a particular case. Problems that still occur today require new innovative methods of flow measurement [6]. Standard orifice flow metres are widely used in the chemical and energy industries [7] as part of the automatic control system. Flue gas ducts usually have measurement ports for inserting Pitot probes, temperature probes and flue gas sampling probes, which are used to measure differential and static pressure, temperature and to determine the composition of the flue gas in a cross-section. The measured values are used to determine the velocity profile in the measurement cross-section and the flow rate by integration. The entire measurement procedure is described by several international standards such as ISO 3966, ISO 10780 or ISO 16911-1. Flow measurement technology has made great strides, but due to its portability, operability and recognised accuracy, the Pitot tube appears to be an acceptable choice for on-site measurement of flue gas velocity in closed ducts when variable flows, complex flue gas composition and large dust particles in the flue gas are present [8, 9].

The measurement of the gas velocity distribution over the entire 14 m × 14 m cross-section of the ESP chamber is a rather challenging task. Particle image velocimetry [10, 11] and laser doppler velocimetry [4] are mainly applicable under laboratory conditions at low gas velocities. The Robinson cup anemometer is not applicable due to its high sensitivity to the position of the rotation axis [12]. The measurement chain of Pitot or Cobra probes with micromanometers may also not be suitable for this type of measurement, since the spatial positioning of the probe is problematic and the measurement chain reaches its limits at velocities of up to several meters per second. In addition, the vibrations and air fluctuations affect the pressure lines, which must be laid over very long distances, or the sensors for static pressure, differential pressure, and temperature measurements must be carried with the probe across the vertical cross-section of the chamber, and a method of transmitting the sensor signals must be provided. Ultrasonic anemometers [13] are not suitable due to their sensitive design and narrow heavy metal structured environment. Despite the robustness of the acoustic resonance anemometer [14] and its applicability in dusty conditions, the use of these sensors for this type of measurement has not been reported yet.

For on-site measurements of air velocity distribution in the large vertical cross-sections of the chambers of ESP, vane [15-17] or hot-wire [18] anemometers are used. Measurements

are usually made by personnel moving the anemometers across the measurement cross-section and recording the velocities at all selected measurement points, or the readings are transmitted to a remote readout/recording unit. This means that personnel have to move over steps and internal ladders and/or other structural elements [19], which is dangerous and tiring. An automated robotic system [17] designed specifically for this type of measurement can be used. However, if the robotic system gets stuck or loses signal, the measurement must be stopped and the flue gas fan (FGF) must be turned off to enter the ESP chamber. After the malfunction is corrected, the FGF must be restarted, creating new flow conditions in the chamber. In many cases, the measurements must be repeated.

For this type of measurements a new transport cart has been developed [20] to transport the hote-wire anemometers. The transport cart is specially designed to be easily mounted on the S-shaped front surface of the collecting electrode (CE) and pushed/rolled up and down by the operators. The anemometers were mounted on the transport cart so that the hot-wire sensors at the tip of the telescopic probe were positioned horizontally in the centre of the gas passage (GP) between two CE. The distribution of the measurement points in horizontal and vertical direction of the chamber cross-section was determined by the inner chamber geometry, the number and width of the GP, but also by the estimated total measurement time.

This paper presents the results of velocity measurements and flow uniformity assessment in the flue gas inlet ducts and in the chambers of ESP of Unit A1. The objective was to capture velocity patterns and identify the main sources of flow non-uniformity. The applied comprehensive analysis based on results of performed measurements and calculated homogeneity parameters reflects the novelty of this work. As a result, a partial reconstruction of the inlet duct was proposed and carried out during the 2020 overhaul. Measurements of flue gas velocity in the ducts were performed before and after the partial reconstruction during the 2020 overhaul, while measurements of air velocity distribution in the vertical cross-sections of the ESP chambers were performed after the reconstruction during the 2020 overhaul.

Problem description

The thermal power of Unit A1 is 633 MWth with 5 mills burning low grade lignite from the Kolubara open pit mine with a capacity of 68 tonne per hour. At the exit from the convective tract of the boiler of Unit A1, the flue gas is divided into two branches leading to two RAPH in the boiler room and then to two ESP chambers behind the boiler room. The flue gas ducts exit the boiler room in a horizontal direction, fig. 1, pos. 1. Due to the 13.2 m height difference between the axis of the horizontal ducts and the axis of the diffusers of the ESP, fig. 1, pos. 7, there is a bend, fig. 1, pos. 3, at the end of the horizontal duct that diverts the flue gas upward into the vertical chamber, fig. 1, pos. 21. The vertical chamber is divided at the top into two parallel vertical ducts, fig. 1, pos. 4, with shut-off vanes behind which there is a elbow with built-in guide vanes, fig. 1, pos. 6, that diverts the flue gasses in the horizontal direction into the diffuser, fig. 1, pos. 7, of the ESP.

The ESP of Unit A1 was rebuilt in 2006 as part of the capital overhaul carried out by ELWO S. A. The enlargement of the ESP chamber resulted in a lateral displacement of the axis of the horizontal flue gas duct at the exit of the RAPH by 550 mm with respect to the axis of the ESP chamber. The position of the two vertical flue gas ducts, fig. 1, pos. 4, with a cross-section of 3 m × 3 m is not symmetrical with respect to the 3 m × 7 m horizontal flue gas duct at the exit of RAPH, fig. 1, pos. 1. Figure 2 shows a top view and fig. 3 a view from the boiler room of the arrangement of the horizontal ducts, fig. 1, pos. 1, vertical ducts, fig. 1, pos. 4, and diffusers, fig. 1, pos. 7, of ESP. It can be seen that in the case of the presented right ESP chamber,

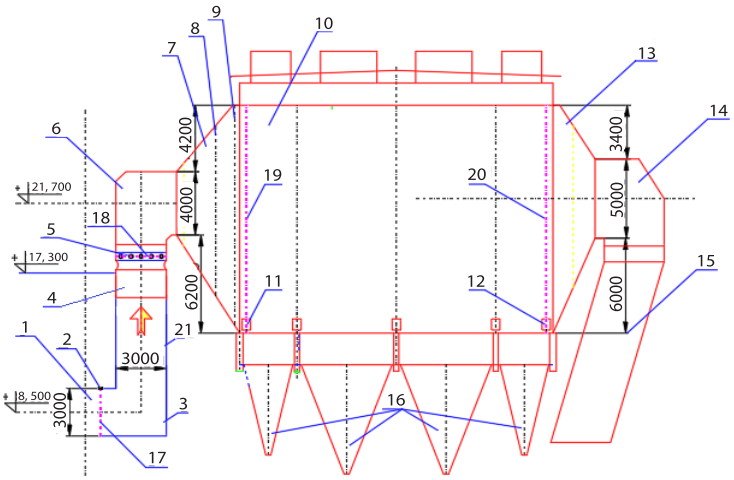

Figure 1. Vertical cross-section of the ESP: *1 – horizontal channel, 2 – position of the measuring openings on the horizontal channel, 3 – horizontal to vertical channel elbow, 4 – vertical channel, 5 – measuring openings on the vertical channel, 6 – elbow inlet to diffuser, 7 – diffuser, 8 – position of the first distribution grate, 9 – position of the second distribution grate, 10 – ESP chamber, 11, 12 – entrance doors, 13 – confusor, 14 – exit elbow, 15 – exit channel to the FGF, 16 – hoppers, 17 – position of the measuring plane on the horizontal channel, 18 – position of the measuring plane on the vertical channel, 19 – position of the measuring plane in the front of first electrical field, 20 – position of the measuring plane behind the fourth electrical field, 21 – vertical chamber*

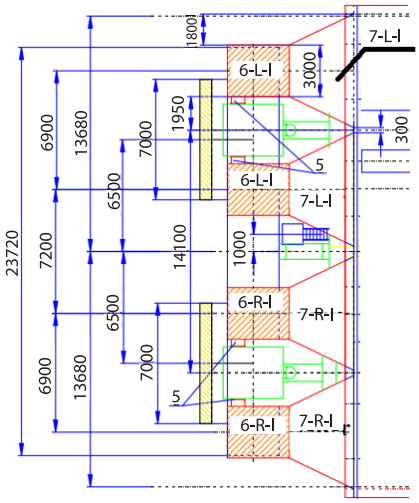

Figure 2. Plan view of the arrangement of channels, fig. 1, pos. 6, and diffusers, fig. 1, pos. 7, at the entrance to ESP (horizontal channels with rectangular cross-section 3 × 7 m – ocher and vertical channels with square cross-section 3 × 3 m – red

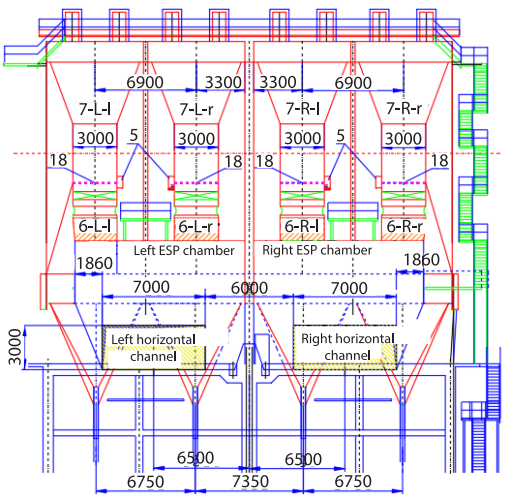

Figure 3. View from the boiler room of the arrangement of the horizontal ducts (ocher) and the vertical ducts (red): left (6 –L-l) and right (6-L-r) vertical channels of the left ESP chamber, left (6 –R-l) and right (6-R-r) vertical channels of the right ESP chamber

the axis of the left vertical duct (marked 6-R-l on fig. 2) and the left diffuser (marked 7-R-l on fig. 2) are within the dimensions of the horizontal flue duct (shown by ocher color), while the axis of the right vertical duct (on fig. 2 marked with 6-R-r) and the right diffuser (marked with 7-R-r in fig. 2) is additionally shifted to the right, *i.e.* outside the dimensions of the horizontal flue duct. For the right ESP chamber the horizontal distance from the axis of the horizontal duct to the axis of the left diffuser is 2900 mm and to the axis of the right diffuser is 4000 mm. The same asymmetry exists for the left ESP chamber, but in reverse order. From the end of the horizontal channel, fig. 1, pos. 1, to the beginning of the vertical channels, fig. 1, pos. 4, there is a vertical chamber, fig. 1, pos. 21, that is 8.75 m high and extends from the bottom of the horizontal channel at a height of 7 m to the beginning of the vertical channels at a height of 15.75 m, fig. 4. The chamber is 3 m deep and has a variable width, ranging from 12.5 m at a height of 7 m to 14.86 m, which corresponds to the chamber width between a height of 11.5 m and 15.75 m. On one of the sides of the vertical chamber there is a bypass channel to the other vertical chamber with shut-off vanes, item (c) on fig. 5. The flow in such a large chamber is very disordered and has many re-circulation flows. Moreover, the irregularity of the velocity field in the vertical chambers is exacerbated by the diagonal plates, item (b) on fig. 5, located in the vertical chamber in front of the entrance to the vertical channels with shut-off vanes, item (a) in fig. 5. These diagonal plates have no proper function and significantly disrupt the flow of flue gas in the vertical chamber.

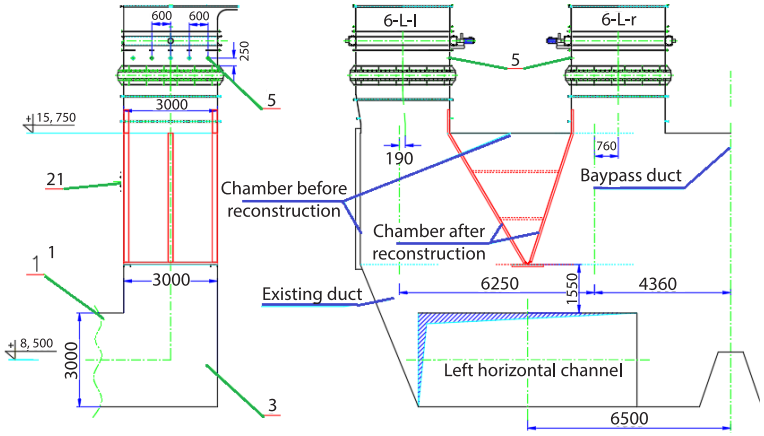

Figure 4. Side (left) and front (from the boiler room) view (right) of the left vertical chamber, black lines – geometry of the chamber before reconstruction, red lines – reconstructed chamber

Unregulated intense flue gas-flow (velocities > 25 m/s) and a high dust concentration (> 70 g/Nm^3) resulted in severe erosion of the metal of the turning vanes in the elbow, fig. 1 pos. 3, downstream of the horizontal ducts, fig. 6(a), turning vanes in the elbow, fig. 1 pos. 6, at the upper end of the vertical ducts, fig. 6(b), but also of the perforated plates in the first distribution grates, fig. 1 pos. 8, of both diffusers. Inspection revealed that damaged perforated plates were replaced with plates of inadequate porosity, as can be notice on fig. 6(c), totaling 16 plates in the first grates in the diffuser of the left ESP chamber and 12 plates in the first grates in the diffusers of the right ESP chamber. The inadequate plates had square openings with a porosity of 62% instead of circular openings with a porosity of 41.6%. Additional asymmetry of flow in the ESP chamber, fig.1, pos 10, is created by the asymmetric position of the exit channel, fig. 1, pos 15, with respect to the vertical axis plane of the ESP chamber. In left ESP chamber, the

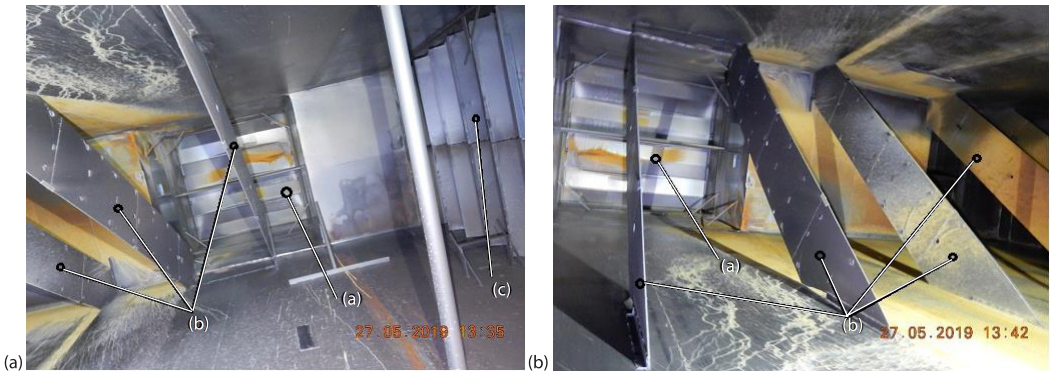

Figure 5. Interior of the left vertical chamber, view from the bottom of the left horizontal channel towards the vertical channels; (a) shut-off vanes in vertical ducts, (b) diagonal panels, and (c) shut-off vanes in bypass duct between left and right vertical chamber

Figure 6. Erosion of the turning vane in the elbow downstream of the horizontal ducts (a), turning vanes in the elbow at the upper end of the vertical ducts (b), and perforated plates in the first distribution grates replaced with plates of inadequate porosity (c)

axis of the channel was shifted to the left by 435 mm, while in the right ESP chamber it was shifted to the right by the same value, fig. 7. Moreover, the axis of the inlet section the diffuser is at a height of 21.7 m, the axis of the duct section at the exit of the confusor, fig. 1, pos 13, is at a height of 22 m, while the axis of the ESP chamber is at a height of 20.2 m. Height asymmetry is common in practice to reduce flue gas velocities in the lower part of the chamber in the back fields and to reduce the amount of particles returned to the gas when the CEs are shaken off, while asymmetry in the width of the ESP chamber is not desirable because it reduces the efficiency of the ESP. Therefore, during the short overhaul of unit A1 in 2020, the following reconstructive intervention was performed only on the left ESP ductwork:

– the "*V*" plates are installed in the left vertical chamber, fig. 4,
– in the first distribution grates of the left, fig. 3 pos. 7-L-l, and right, fig. 3 pos. 7-L-l, diffusers of the left ESP, 8 plates each were replaced, while 10 distribution plates were replaced in the second distribution grate of the left diffuser; the plates with square openings with a porosity of 62% were replaced by plates with circular openings with a porosity of 41.6%, and
– all diagonal panels, fig. 5, pos. (b), were removed.

The proposed reconstructive measures have been agreed with TPP management in accordance with the time and resources available.

Flue gas velocity measurements in horizontal flue gas ducts downstream of the RAPH were made in a vertical cross-section, fig. 1 pos. 17, immediately downstream of the wall of the boiler room. At the top of the duct there are 8 measurement openings, fig. 1 pos. 2,

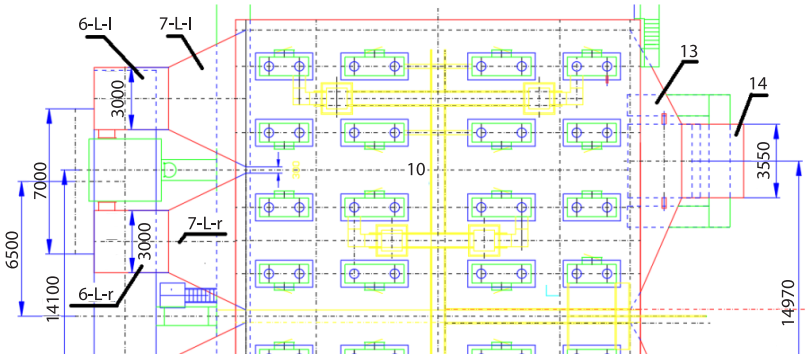

Figure 7. Top wiev of the left ESP: *6 – elbow inlet to diffuser, 7 – diffuser, 10 – ESP chamber, 13 – confusor, 14 – exit elbow, L – left ESP, and l/r – left/right ESP branch*

through which measurements were made at 5 measurement points. Velocity measurements in vertical channels were performed in horizontal cross-sections in front of shut-off vanes, fig. 1 pos. 18, to which 5 measurement ports, fig. 1 pos. 5, were attached. Along each of the measuring axes, 5 measuring points were distributed. In both cases, the distribution of measurement points along the measurement axes was determined according to the requirements of ISO 10780.

Gas velocity measurement was performed on two occasions, before and after partial reconstruction of the left ductwork during the 2020 overhaul. The axial velocity of the flue gas was determined based on differential and static pressure measurements using L-type Paul Gothe pitot probes, which meet all design requirements for AMCA-type dynamic pressure probes in accordance with t. A.2.1.5.1 Annex A of the standard EN ISO 16911-1, and ALNOR AXD560 micromanometers. Flue gas temperature was measured using a thermocouple type-K and digital thermometer PCE T 390.

Flue gas composition was determined using a portable gas analyzer HORIBA PG -350 E. The measurement uncertainty in determining the flue gas velocity was < 3% of the measured values, but greater than 0.1 m/s.

Measurements of the air velocity distribution in the vertical cross-section of the ESP chambers of Unit A1 were performed at the end of the 2020 overhaul, *i.e.*, when the boiler and the unit were out of service. The design value of the flue gas-flow at the nominal power of the unit is 600.8 m^3/s (300.4 m^3/s per ESP chamber), resulting in a design value of the average velocity in the ESP chamber of 1.52 m/s. The intention was to achieve an air volume flow (velocity field) in the ESP chamber as close as possible to the volume flow of the flue gas in nominal operation. Due to differences in air and flue gas density, the FGF speed was gradually increased and at the same time the opening of the deflector blades was adjusted until a velocity of 1.6 m/s was achieved in the 6^{th} flue GP (counting from the wall opposite the door of the chamber) at a height of 3.5 m above the platform. The percentage of opening of the deflector blades was 16% and 17%, while the electrical current of the FGF motor was 129-130 A and 129-131 A for the left and right FGF, respectively. After stable operation of the FGF and a stable air velocity of 1.6 m/s was achieved in the 6^{th} flue GP at a height of 3.5 m above the platform, the FGF parameters were further kept constant throughout the measurement period. The first measurement of the velocity distribution was performed in the right ESP chamber. Then the right FGF was stopped, the team moved to the left chamber of the ESP, the left FGF was started and the measurements were taken in the left ESP chamber. Axial air velocity was measured using TSI Air Pro AP500

hot-wire anemometers with an uncertainty of ±0.1 m/s. Air temperature and humidity were measured using a Pt100 probe and hygrometer built into the AP500 instrument with an uncertainty of ±0.3 °C and ±2.2% RH, respectively. The readings were immediately transmitted via bluetooth, displayed and recorded on the cell phone through the TSI AirPro Mobile software.

The measuring planes for measuring the velocity distribution in the ESP chamber are located before the first, fig. 1 pos. 19, and after the last, fig. 1 pos. 20, dedusting zone. In this measurement section there are control openings, *i.e.* doors for access into the chambers of the ESP. The door provides access to a built-in communications platform for maintenance 13 m above the ground. The operators used these platforms to move along the width of the ESP chamber. In each of the ESP chambers, there are 33 GP with a width of 400 mm (between CE). Velocity measurements were taken in every 3rd GP along the height at 14 measurement points, starting at 0.5 m above the platform and ending at 13.5 m above the platform, so that the area around each measurement point is not larger than 1 m × 1 m. This resulted in a total of 12 × 14 = 168 measurement points in each vertical cross-section and an estimated time of acceptable ~2 hours required for the measurements in one of the ESP chambers. To monitor the change in air-flow through the ESP chamber over time, a control measurement of the air velocity and temperature was made in front of the first electrical zone with a testo 405i anemometer placed at a height of 1.8 m in the GP about 3 m from the wall opposite the door of the chamber. The time between two consecutive measurements was set to 3 seconds.

Homogeneity parameters calculations

The investigation of the uniformity of the flow was performed by examining flow data obtained from field measurements at the cross-sections of interest. To evaluate the homogeneity of the flue gas-flow in the ducts, the coefficient of variation CV [21] is calculated as the ratio of the standard deviation S_{tdev} [ms^{-1}] to the mean gas velocity in the cross-section v_{ave} [ms^{-1}]:

$$CV = \frac{S_{\text{tdev}}}{v_{\text{ave}}} = \frac{1}{v_{\text{ave}}}\sqrt{\frac{\sum_{i=1}^{n}(v_i - v_{\text{ave}})}{n-1}} \tag{1}$$

where n [–] is the number of velocity samples v_i [ms^{-1}]. Since the gas velocity profile in the vertical cross-section of the ESP chamber varies strongly in the vertical and transverse directions, the dimensionless momentum correction Boussinesq coefficient M_k [3] and the energy correction Coriolis coefficient N_k [22] were calculated:

$$M_k = \frac{\int v^2 \mathrm{d}A}{v_{\text{avg}}^2 A_{tot}} = \frac{1}{A_{\text{tot}}}\sum_{i=1}^{n}\left(\frac{v_i}{v_{\text{avg}}}\right)^2 \Delta A_i \tag{2}$$

$$N_k = \frac{\int v^3 \mathrm{d}A}{v_{\text{avg}}^3 A_{tot}} = \frac{1}{A_{\text{tot}}}\sum_{i=1}^{n}\left(\frac{v_i}{v_{\text{avg}}}\right)^2 \Delta A_i \tag{3}$$

where v_i [ms^{-1}] is the average velocity through the elemental area of the cross-section of the ESP chamber, v_{avg} [ms^{-1}] – the average velocity in the cross-section, ΔA_i [m^2] – the elemental area, and n [–] – the number of elemental areas in the cross-section of the ESP chamber. The values of M_k and N_k are equal to one only under uniform flow conditions. Guideline [23] prescribes that in the treatment zone near the inlet and outlet surfaces of the ESP chamber, the velocity pattern should have at least 85% of the velocities no more than 1.15 × v_{avg} and 99% of the velocities no more than 1.4 × v_{avg}.

The relative standard deviation CV as a measure of flow uniformity is useful statistic because it includes velocities < 0.85 × v_{avg}, whereas the guideline [24] focuses only on the high velocities. The metrics of flow uniformity based on the linear L_1 norm [25] and the quadratic L_2 norm [26] were also calculated for the vertical cross-sections of the ESP chamber:

$$\gamma_{L_1} = 1 - \frac{1}{2}\left(\sum_{i=1}^{n} \frac{A_i}{A_{\text{tot}}} \frac{\left|vi - v_{\text{avg}}\right|}{v_{\text{avg}}}\right) \tag{4}$$

$$\gamma_{L_2} = 1 - \frac{1}{2v_{\text{avg}}}\left(\sqrt{\sum_{i=1}^{n} \frac{A_i}{A_{\text{tot}}} (v_i - v_{\text{avg}})^2}\right) \tag{5}$$

where n is the number of cross-sectional subdivisions, i – the cell index, A_i [m^2] – the frontal area of the cell, v_i [ms^{-1}] – the velocity component perpendicular to the cell, tot – the sum, and avg – the area-weighted average. In the case of perfectly uniform flow, γ_{L_1} = 1.0 and γ_{L_2} = 1.0. For the test requirements [23, 24], the additional parameters $A_{<85\%}$, $A_{>115\%}$, and $A_{>140\%}$ were calculated as a percentage of the total area of the cross-section that has velocities < 85%, > 115% and >140% of the mean velocity v_{ave} in the cross-section exhibited.

Results and discussion

The results of the measurement of velocity distribution in the left and right horizontal channels before reconstruction are shown in fig. 8(a) and fig. 9(a), respectively, in the left and right vertical channels of the left ESP are shown in figs. 8(b) and 8(c), respectively, while the results of the measurement of velocity distribution in the left and right vertical channels of the right ESP are shown in figs. 9(b) and 9(c), respectively. The measurement was performed at a constant power of unit of ~120 MW. The average gas velocity v_{ave} [ms^{-1}], flow homogeneity parameter CV [–] and volumetric flow rate Q [m^{3}s^{-1}] for the considered cross-section are shown in tab. 1. The volumetric flow through the left and right horizontal channels differed by a significant 9.2%. Velocity fields are uneven, with higher velocity values near the top and sidewalls of the two horizontal channels.

The volume flow through the left and right vertical channels of the left ESP differed by 5.5%. The velocity fields were uneven, with two main flows of higher velocities, the more intense of which was found near the wall facing the ESP chamber. The relative standard deviation CV, tab. 1, for left channel (0.36) was much higher than recommended value of 0.25

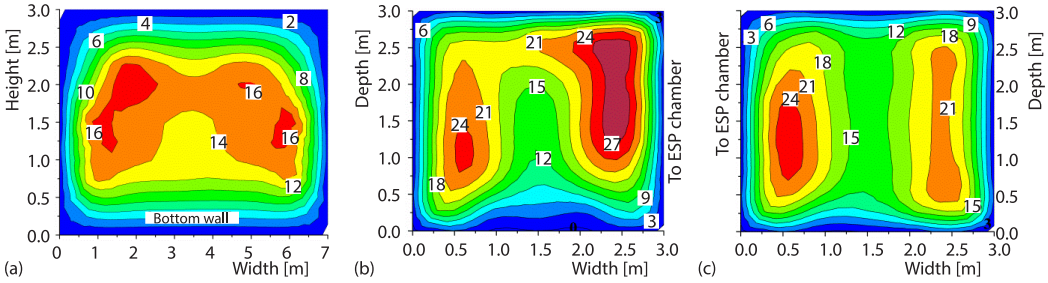

Figure 8. Velocity distribution [m/s] in the left (a) horizontal channel (vertical cross-section pos. 17 on fig. 1, view from the boiler to the ESP chamber), left (b) and right (c) vertical channel of left ESP (horizontal cross-section pos. 5 on fig. 1, top view, before reconstruction

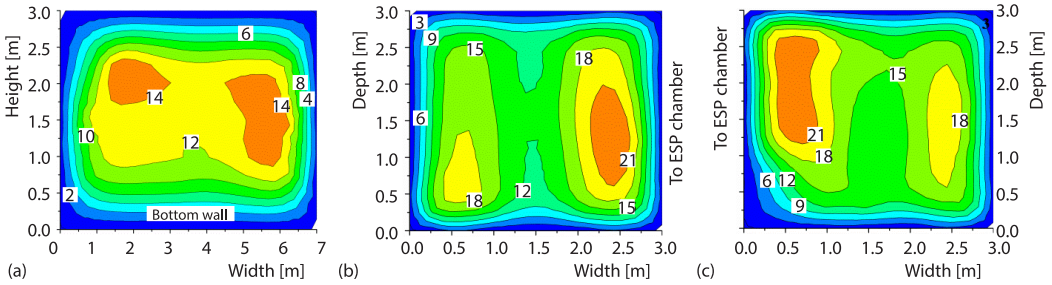

Figure 9. Velocity distribution [ms^{-1}] in the right (a) horizontal channel (vertical cross-section pos. 17 on fig. 1, view from the boiler to the ESP chamber), left (b) and right (c) vertical channel of right ESP (horizontal cross-section pos. 5 on fig. 1, top view) before reconstruction

[22, 23]. The volume flow through the left and right vertical channels of the right ESP differed by 3.1%. The velocity fields were uneven, with two main flows of higher velocities, the more intense of which is located near the wall toward the ESP chamber. The relative standard deviation CV was close to recommended value [22, 23] for both left and right vertical channel. The flows in the horizontal channels were similar to the sum of the flows in the corresponding vertical channels (differing by only 0.6% in the case of the left and 0.7% in the case of the right ESP).

Table 1. The parameters of the flow in the channels

	Left ESP			Right ESP		
Channel	Horizontal	Left vertical	Right vertical	Horizontal	Left vertical	Right vertical
Before reconstruction						
v_{avg} [ms]	13.6	15.5	16.4	12.4	14.4	14.8
CV [–]	0.36	0.36	0.23	0.35	0.23	0.26
Q [m3s^{-1}]	284.9	139.2	147.3	261.0	129.3	133.4
After reconstruction						
v_{avg} [ms^{-1}]	14.0	17.2	16.8	13.1	16.3	15.7
CV [–]	0.37	0.24	0.28	0.39	1.10	0.45
Q [m^{3}s^{-1}]	293.8	154.7	151.0	275.4	147.1	141.3

The results of measuring the velocity distribution in the left and right horizontal channels after reconstruction are shown in figs. 10(a) and 11(a), respectively. The measurement was performed at a constant power of unit of ~120 MW. The difference in volumetric flow through the left and right horizontal channels is decreased up to 6.2%. Flow is relatively uniform in height and width of the two horizontal channels, with higher velocity values near the top of both horizontal channels. In order to correct the velocity profile, the angle of inclination of the deflection blades in the elbow at the end of the horizontal channels should be increased, or a completely new system of deflection vanes should be designed and installed, allowing for a better homogeneity of the flow after deflection.

The results of measuring the velocity distribution in the left and right vertical channels of the left ESP after reconstruction are shown in figs. 10(b) and 10(c), respectively. The flow through the channels is almost the same (it is 2.4% higher in the left vertical channel), regardless of the asymmetry of the axis of the horizontal channel with respect to the axis of the

chamber, *i.e.*, the axis of the left/right vertical channel. The relative standard deviation *CV* is below the recommended value of 0.25 for the left channel and close to it for the right channel. These measurement results clearly show the effectiveness of the reconstructive solution with 2 plates in the shape of the letter V, with which the flow through the vertical chamber is divided and directed into the left/right vertical channel. The velocity fields are still uneven, with two main flows of higher velocities, the more intense of which is located near the walls toward the ESP chamber. This indicates that the turning vanes located in the elbow at the end of the horizontal inlet duct are not properly adjusted to evenly redirect the gas-flow vertically upward to the vertical ducts.

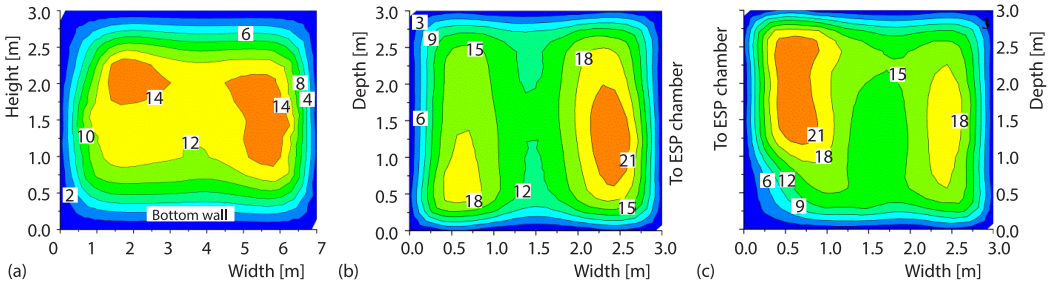

Figure 10. Velocity distribution [m/s] in the left (a) horizontal channel (vertical cross-section pos. 17 on fig. 1, view from the boiler to the ESP chamber), left (b) and right (c) vertical channel of left ESP (horizontal cross-section pos. 5 on fig. 1, top view) after reconstruction

The results of measuring the velocity distribution in the left and right vertical channels of the right ESP after reconstruction are shown in figs. 11(b) and 11(c), respectively. The volume flow through the left and right vertical channels of the right ESP differed by 4.1%. The flow field is extremely uneven in the left channel, with two jets, one of which is very intense with velocities greater than 40 m/s and located along the left channel wall, and the other, smaller jet, located along the right wall of the channel. In almost half of this cross-section of the left channel, the velocity is close to zero. The flow through the right channel is non-uniform with two main flows located near the walls towards the ESP chamber and the boiler, with a significant part of the cross-section having velocities close to zero. The uneven velocity profiles in the vertical channels of the right ESP are a consequence of the pronounced irregularity of the flow in the vertical chamber and the asymmetrical position of the vertical channels in relation to the axis of the horizontal channel. The increased non-uniformity of velocity in vertical channels results in significantly higher local peaks, leading to increased local erosion of both the stop vanes and the turning vanes in the elbow at the top of the vertical channel. The measurements in the chamber were carried out on October 31, 2020, shortly after the first series of velocity measurements in the ducts on September 24, 2020. Due to the COVID -19 regulations, the second series of measurements in the ducts was carried out almost a year after the reconstruction, on August 10, 2021. During this time the A1 unit was in operation without interruption. The inhomogeneous flow with high velocities and dust concentrations led to intense erosion of some turning and structural elements, thus contributing to a further deterioration of the homogeneity of the flow. Local erosion and 10% higher volumetric flow during the second measurement, could be the main reasons for the flow uniformity deterioration when comparing these two measurements, figs. 9 and 11.

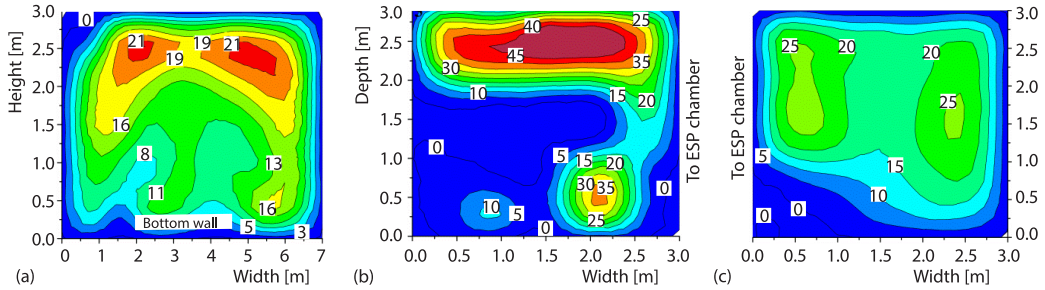

Figure 11. Velocity distribution [ms^{-1}] in the right (a) horizontal channel (vertical cross-section pos. 17 on fig. 1, view from the boiler to the ESP chamber), left (b) and right (c) vertical channel of right ESP (horizontal cross-section pos. 5 on fig. 1, top view) after reconstruction

The results of measuring the velocity distribution in the cross-section of the chambers of ESP before the first electric field are shown in fig. 12, a view from the boiler room to the stack. Figure 13 shows the velocity distribution in the cross-section of ESP after the fourth electric field. The uniformity parameters calculated for vertical cross-sections of the ESP chambers are listed in tab. 2.

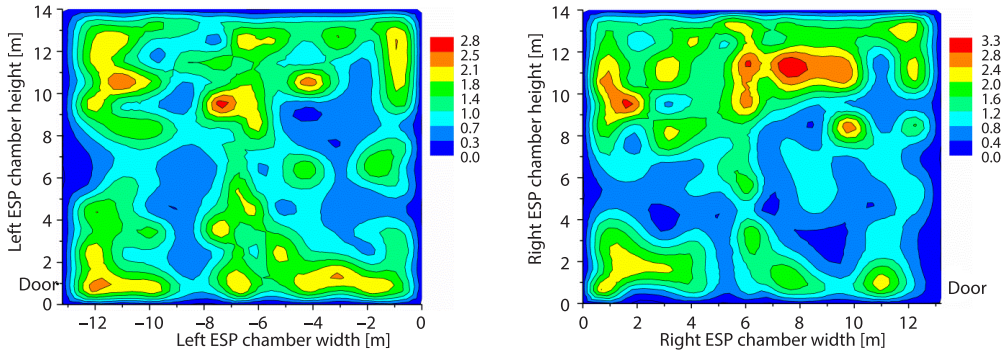

Figure 12. The 2-D representation of the velocity distribution in the front of the 1st electrical field; (a) left ESP chamber and (b) right ESP chamber

The differences in volumetric flue gas-flow through the ducts, tab. 1, compared to volumetric air-flow through the left/right ESP, tab. 2, are an unavoidable consequence of the way the FGF parameters and the degree of flap openings were adjusted for the measurements in each of the ESP chambers. The total volume flow of air through the left/right ESP chamber was calculated from the measurement results by integrating the velocities over the associated areas. The average velocity was 23% and 16% below the design value of 1.52 m/s when measured

Table 2. The uniformity of the flow in the vertical cross-sections of the ESP chambers

Parameter	Q [m^{3}s^{-1}]	v_{avg} [ms^{-1}]	v_{max}/v_{avg} [–]	M_K [–]	N_K [–]	L_1 [–]	L_2 [–]	CV [%]	$A_{<85\%}$ [%]	$A_{>115\%}$ [%]	$A_{>40\%}$ [%]
Recomendation	–		–	≤1.2	≤1.8	~ 1.0	~ 1.0	≤25%	≤25%	≤25%	≤5%
Left ESP inlet	224.0	1.17	2.39	1.31	2.00	0.81	0.75	46.44	39.1	35.9	24.2
Right ESP inlet	245.1	1.28	2.54	1.38	2.26	0.78	0.72	53.67	37.6	40.5	25.3
Left ESP outlet	213.9	1.12	2.36	1.46	2.56	0.76	0.69	63.12	27.6	22.4	16.1

in the left and right ESP chambers, respectively. The control velocity measurements indicate a very stable air-flow during the measurements, with a standard deviation around the mean of 0.23 m/s and 0.21 m/s for the left and right ESP chamber, respectively, and recorded min/max values of 1.7/3.2 m/s and 1.6/2.7 m/s for the left and right ESP chamber, respectively.

In the case of the left ESP chamber, the higher velocities occurred at the bottom, sides, near the top, and in the central vertical axial plane of the left chamber where the two diffusers meet, fig. 12(a). The measurements also indicate uneven air-flow through the left/right half of the chamber at its initial cross-section, but in contrast to the expected, increased air-flow through the right diffuser (right half of the ESP chamber according to the original documentation). The percentage of air-flow through the left half of the chamber, *i.e.*, through the left diffuser, was 52.2% and through the right diffuser was 47.8%. These data indicate that the ESP reconstruction during the 2020 overhaul mitigate the vertical duct asymmetry problem.

The results of the measurement of the velocity distribution in the cross-section before the first electric field of the right ESP chamber are shown in fig. 12(b). Similar to the left ESP chamber, the higher velocities occurred at the bottom, sides, near the top, and in the mid-vertical axial plane of the left chamber (where the two diffusers meet). The flow through the left/right half of the right ESP chamber is uneven in its initial cross-section. The percentage of flow through the left half of the chamber, *i.e.*, the left diffuser, is 54.3% and through the right half is 45.7% of the total flow.

This is primarily a consequence of the asymmetry of the distance of the vertical channels from the axis of the horizontal inlet channel. The velocity distribution in the left, fig. 12(a) and especially in the right ESP chamber, fig. 12(b) is characterized by numerous velocity peaks (up to 3.3 m/s in the right and below 2.8 m/s in the left chamber). As a result of the reconstructions performed during the 2020 overhaul for the left ESP chamber only, the relative standard deviation of 46.4% for the left ESP chamber shows a slightly better velocity distribution at the beginning of the chamber compared to the value of 53.6% for the right ESP chamber, tab. 2.

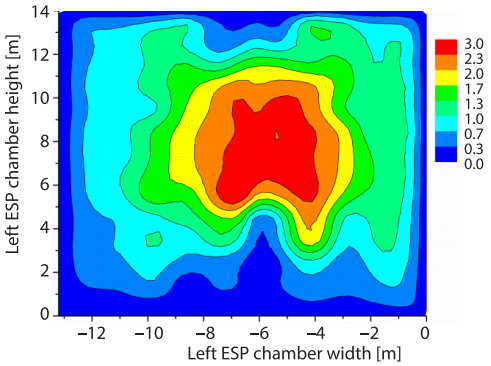

Figure 13. The 2-D representation of the velocity distribution behind 4th electrical field of the left ESP chamber

The asymmetry of the flow that occurs immediately at the exit of the RAPH, *i.e.* at the entrance to the horizontal channels (cross-section marked as pos. 17 on fig. 1), is shown in figs. 8(a)-11(a). The system of turning vanes in the elbow pos 3 fig. 1 cannot correct this asymmetry, which is exacerbated by the asymmetrical position of the horizontal ducts in relation the vertical chamber and the asymmetry of the vertical chamber itself. The asymmetry of the flow is further transmitted through the vertical ducts, figs. 8-11, and the diffuser into the ESP chamber, where neither the system of turning vanes in the elbow at the diffuser inlet, pos. 6, fig. 1 ,nor the system of perforated plates in the diffuser, pos. 8 and 9, fig. 1, can compensate for the asymmetry to a sufficient degree. Finally, it manifests itself in the form of a zone of increased velocities along the ceiling of the ESP chamber, fig. 12.

The measurement of the velocity distribution in the cross-section behind the fourth electric field of the left ESP chamber was performed simultaneously with the measurement of the velocity distribution before the first electric field in the left ESP chamber. The measurements were carried out simultaneously by two teams and two sets of equipment under the

same flow conditions at the entrance to the ESP chamber. Measurements indicated uneven flow through the left/right halves of exit section of the ESP chamber. The flow through the left and right halves of the chamber was 46.9% and 53.1%, respectively. The good agreement of the measured flow (*i.e.*, calculated mean velocities of 1.17 and 1.12 m/s) in the cross-sections upstream of the first, fig. 12(a) and downstream of the fourth electric field, fig. 13, of the left ESP chamber indicates a high quality of the measurements. For the velocity distribution in the last zones of ESP the influence of FGF on the flow through the central exit opening is dominant. The distribution grate in the confusor does not have the expected positive effect for the formation of a uniform flow distribution, especially along the chamber width. As a result, dust collection performance in the last electrical zones of the ESP is also impaired.

The homogeneity parameters calculated on the basis of eqs. (1)-(3) and tested against the requirements of the guidelines [23, 24] are listed in tab. 2 for all cross-sections of interest. In addition, the volumetric flow rate Q, the relative standard deviation CV, and the percentage of the cross-section $A_{<85\%}$, $A_{>115\%}$, and $A_{>140\%}$ with velocities < 85%, > 115%, and > 140% of the value of the mean velocity in the cross-section v_{avg} are also given.

The calculated homogeneity parameters indicate that the velocity fields in both chambers show unsatisfactory homogeneity for all parameters considered. The results of the measurements and the analysis of the flow homogeneity show that the velocity distribution in the left and especially in the right ESP chamber is very non-uniform, both in terms of span and chamber height. As a result, the ESP has a significantly reduced PM dedusting efficiency.

Conclusions

Velocity distribution and flow homogeneity were evaluated in the flue gas ducts and chambers of ESP of Unit A1. The measurements of the velocity distribution in the flue gas ducts showed a pronounced inhomogeneity of the velocity field. The main causes of the inhomogeneity were determined to be the asymmetric position of the horizontal and vertical ducts upstream of the diffuser and the asymmetric position of the duct at the exit of the confusor with respect to the axis of symmetry of ESP. During the 2020 overhaul, the vertical chamber in front of the left ESP is reconstructed so that the flat top wall of the duct the shape of a "*V*". The results of velocity measurements in the ducts have shown that the difference of flow values through the left/right channel decreased from 5.5-2.4% and the value of relative standard deviation CV decreased to 0.24 and 0.28 for the left/right channel, respectively. This indicates that the reconstruction improved the homogeneity and thus alleviated the problem of the asymmetry of the vertical ducts of the left ESP. The flow field in the unreconstructed right ESP ductwork remains highly uneven, especially in the left vertical channel, with velocities in excess of 40 m/s leading to increased local erosion of stop vanes and the turning vanes. Notwithstanding the positive effects of reconstruction on the flow field in the channels of the left ESP, the value of the relative standard deviation CV for each of the two horizontal and four vertical channels is still higher than the recommended 0.25. Therefore, additional measures should be taken to improve the homogeneity of the velocity field in the channels.

By using new transport trolleys for anemometers, reliable velocity measurements were achieved in large vertical cross-sections of the chamber (13.7 m × 13.5 m). The accuracy achieved is reflected in the fact that the measured flows through the section in front of the first electric field and through the section behind the fourth electric field differ by 4.5%. The homogeneity parameters are evaluated for vertical cross-sections before the first electric fields in the left and right chambers and for the cross-section after the last electric field in the left ESP chamber. The Boussinesq coefficient were determined to be 1.31 and 1.38, and the Coriolis co-

efficient 2.0 and 2.26 for the left and right chambers, respectively. For the cross-section behind the last electric field of the left ESP chamber, these coefficients were calculated as 1.46 and 2.56, respectively. The linear and quadratic norm-based uniformity parameters were calculated for all cross-sections with less than 0.8 and a relative standard deviation greater than 45%. The results of the measurements of the velocity distribution in the chambers, supported by the results of the analysis of the homogeneity parameters calculated for these cross-sections, clearly showed a pronounced non-uniformity of the flow field with respect to all the recommended criteria. Despite the positive effects achieved by the changes at the entrance of the left ESP during the overhaul of Unit A1 in 2020, they are insufficient and it is necessary to significantly improve the flow field in the chambers to achieve the required level of homogeneity for maximum dedusting efficiency. The problems of velocity peaks and increased flow in the upper and lower regions in both the left and right chambers of the ESP must be solved to improve the dust removal efficiency of the ESP. Future reconstructive measures may include some or all of the following: the installation of new turning vanes in the bend at the end of the vertical ducts, a new system of guide plates at the beginning of the diffuser, the reconstruction of distribution grates with a different arrangement of plate porosity, the installation of new horizontal and vertical guide plates between the distribution grates, the reconstruction of the distribution grate in the confusor and the installation of turning vanes in the elbow at the exit of the ESP chamber.

Acknowledgment

The authors would like to acknowledge their high appreciation the Ministry of Science, Technological Development and Innovation of the Republic of Serbia (Project No. III42010 *Reduction of Air Pollution from Thermal Power Plants of the PE Electric Power Industry of Serbia*, research theme *Improving the efficiency of equipment for waste gas purification and exploitation processes by increasing the fuel quality and assessing the impact on air pollution* which is being realized in VINČA Institute of Nuclear Sciences – National Institute of the Republic of Serbia, University of Belgrade, Belgrade, Serbia), as well as to Joint stock company *Elektroprivreda Srbije*, Belgrade, Serbia (Contract No. 105-E.03.01-72412/11-2020).

References

[1] Daniele, S., *et al.*, Mitigation Strategies for Reducing Air Pollution, *Environmental Science and Pollution, 27* (2020), Apr., pp. 19226-19235
[2] Kiss, F. E., Petkovič, Đ. P., Revealing the Costs of Air Pollution Caused by Coal-Based Electricity Generation in Serbia, *Proceedings*, 7th Exploitation of Renewable Energy Sources and Eciency EXPRES 2015, Subotica, Serbia, 2015, pp. 96-101
[3] Jedrusik, M., *et al*., Physical and Numerical Modelling of Gas-Flow in Electrostatic Precipitator, *Przeglad Elektrotechniczny*, *93* (2017), 2, pp. 228-231
[4] Grainger, C., Paulson, C., Ductwork Changes Improve ESP Performance: Relatively Inexpensive Changes Improve Velocity Distribution throughout the Electrostatic Precipitator, Which Drastically Reduces Particulate Emissions, (Environmental Manager), *Chemical Engineering*, *110* (2003), 1, 69
[5] Cleland, N. A., Aziz, K., A Report on Gas-flow Measurement, (CIM·AIME Petroleum Engineering Section Study Group, Edmonn, 1961/2), *Journal of Canadian Petroleum, Technology*, *2* (1962), pp. 130-152
[6] Krasnov, A. N., Prakhova, M. Y., Instantaneous Gas-Flow Rate Estimation in the Gasgathering System Flowline by Indirect Measurement Method, *Journal Phys. Conf. Ser.*, 1889 (2021), 052045
[7] Anna, G. J., *et al*., Determination of the Uncertainty of Mass-Flow Measurement Using the Orifice for Different Values of the Reynolds Number, *Proceedings*, EFM 2018, EPJ Web of Conferences 213, 2019, 02022
[8] Care, I., Fourneaux, F., Investigation of the Pressure Response of Different Pitot Tubes, Flow Measurement and Instrumentation, *72* (2020), 101714
[9] Butterfield, D., Robinson R., A Study of the Measurement Issues Associated with the Monitoring of Gaseous Emissions from Industrial Plants, NPL Report DQL-AS 022, National Physical Laboratory, Teddington, UK, 2005

[10] Dongjie, Y., *et al*., The 3-D-PIV Measurement for EHD Flow of Spiked Tubular Electrode Corona Discharge in Wide Electrostatic Precipitator, *Measurement Science Review*, *20* (2020), 4, pp. 178-186
[11] Podlinski J., *et al.*, Measurement of the Flow Velocity Field in Multi-Field Wire-Plate Electrostatic Precipitator, *Czechoslovak Journal of Physics*, *54* (2004), Suppl. C, pp. C922-C930
[12] Brevoort, M. J. Joyner, U. T., Experimental Investigation of the Robinson-Type Cup Anemometer, NACA-TR-513, National Advisory Committee for Aeronautics, Langley Memorial Aeronautical Laboratory, Langley Field, Va., USA, 1935
[13] Camuffo, D., Chapter 20 – Measuring Wind and Indoor Air Motions, in: *Microclimate for Cultural Heritage*, 3rd ed., Measurement, Risk Assessment, Conservation, Restoration, and Maintenance of Indoor and Outdoor Monuments, Elsavir, Amsterdam, The Netherlands, 2019, pp. 483-511
[14] Kapartis, S., Anemometer Employing Standing Wave Normal to Fluid-flow and Travelling Wave Normal to Standing Wave, United States Patent, Patent Number: 5,877,416, Date: Mar. 2, 1999
[15] Paulraj, P. A. *et al*., System and Method for Gas Distribution Measurement for Electrostatic Precipitator, United States Patent Application Publication, Pub. No.: US 2012/0279293 A1, Pub. Date: Nov. 8, 2012
[16] Steiner, D.*, et al.*, Influence of Gas Distribution, Field Velocity and Power Supply Technique for Small Scale Industrial ESP's, *International Journal of Plasma Environmental Science and Technology*, *5* (2011), 2, pp. 124-129
[17] Xiang, X., *et al.*, Collection Enhancement Mechanism and Test of Side-flow Electrostatic Precipitation, *Aerosol and Air Quality Research*, *20* (2020), 4, pp. 844-851
[18] Vaddi, R. S., *et al*., Behavior of Ultrafine Particles in Electro-Hydrodynamic Flow Induced by Corona Discharge., *Journal Aerosol Sci*., *148* (2020), 105587
[19] Marković, Z., *et al*., Problem of Gas Distribution in Electrostatic Precipitators of Unit A4 in TPP Nikola Tesla, SimTerm 2019, *Proceeding*s, 19th Conference on Thermal Science and Engineering of Serbia, Sokobanja, Serbia, 2019, pp. 470-485
[20] Lazović, I., *et al.*, Transport Trolleys for Anemometers for Testing the Air Velocity Profile in the Chambers of Electrostatic Precipitators of Large Emitters (in Serbian), Petty Patent No. 1775, Intellectual Property Gazette No. 11, The Intellectual Property Office of the Republic of Serbia, 2022, pp. 46
[21] Zhao, D., *et al.*, Flow Field Simulation and Optimization Design of SCR of 660 MW Power Unit Based on CFD, I*OP Conf. Ser.: Earth Environ. Sci*., *170* (2018), 042031
[22] Zhou, J., *et al.*, Energy and Momentum Correction Coefficients Within Contraction Zone in Open-Channel Combining Flows, *Water Science and Engineering*, *14* (2021), 4, pp. 337-344
[23] ***, Electrostatic Precipitator Gas-flow Model Studies, Publication ICAC-EP-7, Institute of Clean Air Companies, Washington, USA, 2004
[24] ***, VDI 3678 Part 1, Electrostatic Precipitators – Process and waste gas cleaning, VDI/DIN-Handbuch Reinhaltung der Luft, Band 6: Abgasreinigung – Staubtechnik Beuth Verlag, Berlin, Germany, 2011
[25] Ngo, T. T., *et al*, Enhancement of Exit Flow Uniformity by Modifying the Shape of a Gas Torch to Obtain a Uniform Temperature Distribution on a Steel Plate During Preheating, *Applied Sciences*, *8* (2018), 11, 2197
[26] Munnannur, A., *et al*., Development of Flow Uniformity Indices for Performance Evaluation of Aftertreatment Systems, *SAE Int. J. Engine*s, *4* (2011), 1, pp. 1545-1555

Paper submitted: August 16, 2023
Paper revised: October 16, 2023
Paper accepted: October 26, 2023